Journal of the Oman Medical Association

MDPI

Article

Virulence Determinants of Urinary *Pseudomonas aeruginosa* Clinical Isolates: A Phenotypic and Genotypic Study

Mohammed Irmayyidh Mutar [1], Velayuthaprabhu Shanmugam [1,*], Priyanka Preethi [1], Vijaya Anand Arumugam [2] and Manoj Mani [2]

[1] Department of Biotechnology, Bharathiar University, Coimbatore 641046, Tamil Nadu, India; mo7mod.2016@gmail.com (M.I.M.); rpriyanka.phd@gmail.com (P.P.)
[2] Department of Human Genetics and Molecular Biology, Bharathiar University, Coimbatore 641046, Tamil Nadu, India; avahgmb@buc.edu.in (V.A.A.); manojinthravathi@gmail.com (M.M.)
* Correspondence: velayuthaprabhu@buc.edu.in; Tel.: +91-9994240306

Abstract

This study aimed to characterize antimicrobial resistance, biofilm formation, and phenotypic and genotypic virulence-associated traits in urinary *P. aeruginosa* isolates in Iraq. Methods: Twenty *P. aeruginosa* isolates recovered from 100 urine samples from patients with urinary tract infections at Al-Ramadi Teaching Hospital, Anbar, Iraq, were characterized using conventional biochemical tests and the VITEK® 2 automated system. The expected 16S rRNA gene amplicon was assessed in all isolates; sequencing and phylogenetic analysis were performed on four selected isolates. Biofilm formation was assessed using the crystal violet microtiter plate, tube adherence, and Congo red agar methods. Antimicrobial susceptibility was tested by Kirby–Bauer disk diffusion using CLSI M100, 35th edition (2025), and the multiple antibiotic resistance (MAR) index was calculated using six antimicrobial agents. Phenotypic assays assessed capsule-associated extracellular polysaccharide production, protease, lecithinase, coagulase, hemolytic and pyocin activity, pigment production, and adhesion to human uroepithelial cells. PCR was used to detect *algD*, *lasR*, *oprD*, and *mexB*. Separately, a retrospective review of 188 urine-culture records from 2025 identified 131 culture-positive specimens. Results: All 20 isolates were identified as *P. aeruginosa* and met the study's MDR criterion. MAR indices ranged from 0.33 to 1.00. All isolates formed biofilms; by the crystal violet assay, four (20%) were strong producers and 16 (80%) were moderate producers. Capsule-associated extracellular polysaccharide production, protease activity, β-hemolysis, and pyocin activity were detected in all 20 isolates. Pyocyanin was detected in 16 (80%) isolates, and pyoverdine was detected in seven (35%) isolates. Adhesion indices ranged from 4.3 to 19.5 bacteria per cell, with 11 (55%) isolates classified as high-adherence. PCR detected all four target regions in all isolates, although target detection alone does not establish gene expression or function. In the separate retrospective survey, *E. coli* was the most frequently reported organism (27.5%), and *P. aeruginosa* accounted for 7.6% of positive cultures. Conclusions: These findings support local resistance surveillance, susceptibility-guided treatment, and infection-control measures. Larger studies linking molecular, phenotypic, and patient-level outcomes are needed.

Keywords: *Pseudomonas aeruginosa*; urinary tract infection; virulence factors; biofilm; multidrug resistance; antimicrobial resistance

Check for updates

Academic Editor: Rashid Al Abri

Received: 8 June 2026
Revised: 29 October 2026
Accepted: 4 November 2026
Published: 10 November 2026

Copyright: © 2026 by the authors. Published by MDPI on behalf of the Oman Medical Association. Licensee MDPI, Basel, Switzerland. This article is an open access article distributed under the terms and conditions of the Creative Commons Attribution (CC BY) license.

1. Introduction

Urinary tract infections (UTIs) are among the most prevalent infectious diseases worldwide and are a major cause of morbidity in community and healthcare settings, particularly among catheterized, critically ill, and immunocompromised patients [1]. Although *Escherichia coli* is the predominant uropathogen, *Pseudomonas aeruginosa* is a clinically important cause of complicated and catheter-associated UTIs (CAUTIs) and is associated with treatment challenges, prolonged hospitalization, and recurrence [2,3]. Its antimicrobial resistance and diverse virulence mechanisms make it an important pathogen for local clinical characterization.

The pathogenic significance of *P. aeruginosa* reflects its intrinsic antimicrobial resistance, capacity to acquire additional resistance determinants, and diverse virulence mechanisms [4,5]. Biofilm formation can contribute to persistence and reduced antimicrobial susceptibility through matrix-associated protection and physiological heterogeneity. The *algD* gene encodes GDP-mannose dehydrogenase, an enzyme involved in alginate biosynthesis; however, detection of *algD* alone does not establish alginate production, a mucoid phenotype, or biofilm formation [6].

Virulence regulation in *P. aeruginosa* involves quorum-sensing systems. The Las system, regulated by *LasR*, influences the expression of several secreted virulence factors and biofilm-associated traits [7]. Resistance mechanisms include efflux-pump activity, including the MexAB–OprM system, whose *MexB* component is an RND-family transporter encoded by *mexB*; reduced carbapenem uptake may also occur through loss, mutation, or downregulation of the *OprD* porin [8,9]. Detection of the corresponding genes does not, by itself, establish their expression or functional activity.

Additional virulence contributors include pyocyanin-mediated host oxidative damage, pyoverdine-facilitated iron acquisition, extracellular proteases, hemolysins, and uroepithelial adhesins that initiate colonization and biofilm establishment on mucosal surfaces and indwelling urinary devices [10,11].

Despite the clinical importance of *P. aeruginosa* in UTIs, studies integrating comprehensive phenotypic and genotypic characterization of urinary isolates, particularly from Middle Eastern clinical settings, remain scarce. Epidemiological surveillance data from Anbar Governorate, Iraq, are especially limited despite a documented high burden of antimicrobial resistance in this region [12,13].

This study aimed to characterize urinary *P. aeruginosa* isolates from Al-Ramadi Teaching Hospital using conventional identification, VITEK® 2, antimicrobial susceptibility testing, phenotypic virulence assays, and PCR detection of selected targets (*lasR*, *algD*, *oprD*, and *mexB*) [14,15]. The expected 16S rRNA gene amplicon was assessed in all isolates, while sequence-based phylogenetic confirmation was performed on a selected subset. A separate retrospective survey used the hospital bacteriology unit records for 2025 to describe the local epidemiological profile of urine-culture findings.

2. Materials and Methods

2.1. Study Design

This cross-sectional laboratory study was conducted at Al-Ramadi Teaching Hospital, Anbar, Iraq. Urine samples from clinically diagnosed UTI patients were referred to the microbiology laboratory by consultant physicians from the internal medicine, urology, and nephrology wards. Of 100 samples processed, 20 (20%) yielded confirmed multidrug-resistant (MDR) *P. aeruginosa* isolates.

The study comprised two distinct components. The first was a laboratory-based investigation involving 100 urine samples, from which 20 clinical *Pseudomonas aeruginosa* isolates were recovered and characterized phenotypically and genotypically. The second was a

retrospective epidemiological survey of 188 urine-culture specimens recorded at Al-Ramadi Teaching Hospital, Anbar, Iraq during 2025, of which 131 yielded positive cultures. These components were analyzed independently, and their respective sample sizes, denominators, and findings were kept separate throughout the study.

2.2. Ethical Considerations

Ethical approval was obtained from the University of Anbar Ethics Committee (Approval No. 257, 26 December 2024). Informed consent was obtained from all participants, and full patient confidentiality was maintained throughout the study.

2.3. Sample Collection and Processing

Fresh urine samples were collected in sterile containers under aseptic conditions. Samples were gently mixed and inoculated onto blood agar and MacConkey agar using a calibrated loop (0.001 mL) to allow semi-quantitative assessment of bacteriuria. Plates were incubated aerobically at 37 °C for 18–24 h, and colony counts $\geq 10^5$ CFU/mL were considered significant bacteriuria in the appropriate clinical context.

2.4. Biochemical Characterization and Automated Identification

Presumptive isolates were subjected to a panel of conventional biochemical tests, including oxidase, catalase, citrate utilization, triple sugar iron (TSI) reaction, nitrate reduction, urease, indole, Voges–Proskauer, DNase, starch hydrolysis, and growth on cetrimide agar. The characteristic biochemical pattern, oxidase-positive, catalase-positive, citrate-positive, alkaline TSI slant without gas or H_2S production, positive nitrate reduction, and negative reactions for indole, urease, and DNase, supported identification as *P. aeruginosa* [16,17].

For confirmatory identification, all presumptive isolates were processed with the VITEK® 2 automated identification system (bioMérieux, Inc., Durham, NC, USA) using the GN identification card, according to the manufacturer's instructions [18]. Isolates with high-probability identification as *P. aeruginosa* were included in the study and designated PA1–PA20. The reference strain *P. aeruginosa* ATCC 15442 was used as a quality control throughout all experiments.

2.5. 16S rRNA Gene Amplification and Sequencing of Selected Isolates

Genomic DNA was extracted from overnight cultures of each isolate using the Geneaid kit [19]. DNA quality was assessed by electrophoresis on a 0.8% agarose gel. The 16S rRNA gene was amplified from all 20 isolates using universal primers, with an expected amplicon size of approximately 450 bp. PCR products were separated on a 1.2% agarose gel containing ethidium bromide and visualized under UV transillumination [20].

Sanger sequencing was performed on four selected amplicons to provide additional sequence-based confirmation. The phylogenetic tree displays four selected clinical isolates labelled S1, S4, S6, and S14, as shown in the sequencing dataset. Sequences were compared with reference sequences in the NCBI database using BLAST + (Version 2.17.0), and a Neighbor-Joining tree with 1000 bootstrap replicates was generated in MEGA 11 [21]. Conventional biochemical tests and VITEK® 2 were used to identify all 20 isolates; the sequence-based analysis should be interpreted as confirmation of the selected subset rather than all 20 isolates.

2.6. Antimicrobial Susceptibility Testing

Antimicrobial susceptibility testing was performed using the Kirby–Bauer disk-diffusion method on Mueller–Hinton agar (MHA), following the Clinical and Laboratory Standards Institute (CLSI) recommendations for *Pseudomonas aeruginosa* (CLSI M100, 35th

edition, 2025) [22]. Briefly, bacterial suspensions were prepared in sterile saline and adjusted to a turbidity equivalent to a 0.5 McFarland standard. The suspensions were uniformly inoculated onto MHA plates to obtain a confluent bacterial lawn. Commercial antibiotic disks were then applied, including amikacin (AK, 30 µg), aztreonam (ATM, 30 µg), piperacillin (PRL, 100 µg), imipenem (IPM, 10 µg), gentamicin (CN, 10 µg), ciprofloxacin (CIP, 5 µg), netilmicin (NET, 30 µg), and ceftazidime (CAZ, 30 µg). The plates were incubated at 37 °C for 16–18 h. Subsequently, the diameters of the inhibition zones, including the antibiotic disks, were measured in millimetres. Susceptibility results were categorized as susceptible (S), intermediate (I), or resistant (R) according to the applicable CLSI interpretive criteria.

Isolates were classified as multidrug-resistant (MDR) if they exhibited non-susceptibility to at least one antimicrobial agent in three or more antimicrobial categories, in accordance with the consensus definition proposed by Magiorakos [23,24]. For MDR classification, non-susceptibility included both intermediate and resistant results. Antimicrobial categories, rather than the number of individual agents, were considered when applying this definition.

The multiple antibiotic resistance (MAR) index was calculated for each isolate using the following formula:

$$\text{MAR} : \frac{(a)}{(b)}$$

where a represents the number of antimicrobial agents included in the MAR calculation to which the isolate was classified as resistant, and b represents the total number of antimicrobial agents included in the calculation. In the present study, six antimicrobial agents (amikacin, aztreonam, piperacillin, imipenem, ciprofloxacin, and ceftazidime) were included; therefore, b = 6. Only resistant results were counted in the numerator, whereas intermediate results were not counted as resistant. Accordingly, the MAR index for each isolate was calculated by dividing the number of resistant results among these six agents by six. Gentamicin (CN) was not assigned an S/I/R category because CLSI M100-Ed35 (2025) does not provide disk-diffusion interpretive breakpoints for *P. aeruginosa*. Netilmicin (NET) was interpreted using the applicable CLSI M100-Ed35 criteria but was excluded from the MAR calculation because the index was defined using the six agents listed above.

2.7. Quantitative and Qualitative Biofilm Assays

Biofilm formation was assessed using three complementary methods to ensure reliability and reproducibility.

2.7.1. Crystal Violet Microtiter Plate Assay

Biofilm-forming capacity was quantified using the crystal violet (CV) microtiter plate assay as described by Stepanovic et al. (2000) [25] with minor modifications, using *P. aeruginosa* ATCC 15442 as a reference control strain. Overnight cultures were adjusted to 0.5 McFarland standard (~1×10^8 CFU/mL) and diluted 1:100 in fresh TSB to yield a working inoculum of ~1×10^6 CFU/mL. Aliquots of 200 µL were dispensed in triplicate into sterile 96-well flat-bottom polystyrene microtiter plates alongside sterile TSB negative controls, and incubated statically at 37 °C for 24 h. Following incubation, planktonic cells were removed by washing three times with PBS (pH 7.4), and adherent biofilms were stained with 0.1% CV for 15 min. After washing with distilled water and air-drying, the bound dye was solubilized in 95% ethanol, and optical density was measured at 570 nm (OD_{570}) using a microplate reader.

The optical density cut-off value (ODc) was calculated as:

$$\text{ODc} = OD\ control + 3 \times SDcontrol$$

where ODc represents the optical-density cut-off used for biofilm classification, OD represents the optical-density measurements from the negative-control wells, and SD represents the standard deviation of those measurements. Isolates were categorized as non-biofilm producers ($OD_{570} \leq ODc$), weak producers ($ODc < OD_{570} \leq 2 \times ODc$), moderate producers ($2 \times ODc < OD_{570} \leq 4 \times ODc$), or strong producers ($OD_{570} > 4 \times ODc$).

2.7.2. Tube Adherence Assay

Glass tubes containing TSB were inoculated with test isolates and incubated at 37 °C for 24 h. After decanting the broth, tubes were washed with PBS, stained with 0.1% CV for 15 min, and rinsed to remove excess dye. Visible film lining the tube wall and bottom was recorded as biofilm-positive, and intensity was graded qualitatively as: (−) no film, (+) weak, (++) moderate, (+++) strong, in concordance with microtiter results [17,26].

2.7.3. Congo Red Agar (CRA) Method

CRA plates were prepared using brain–heart infusion agar (37 g/L) supplemented with 5% sucrose and 0.08 g/L Congo red dye. Isolates were streaked and incubated at 37 °C for 24–48 h. Black, dry, crystalline colonies were interpreted as indicative of strong biofilm-associated exopolysaccharide production, whereas red or pink colonies were classified as weak or non-biofilm producers [17,27].

2.8. Phenotypic Detection of Capsule-Associated Extracellular Polysaccharide Production

Capsule-associated extracellular polysaccharide production was assessed using India ink negative staining to visualize capsule-associated material [6]. A drop of 6% glucose solution was mixed with bacterial culture, followed by a drop of India ink. The mixture was spread into a thin film, air-dried, fixed with methanol, and stained with methyl violet for 1–2 min. After rinsing with distilled water, the slide was examined under oil-immersion microscopy. A clear halo surrounding stained bacterial cells was interpreted as positive for capsule-associated extracellular polysaccharide. This method does not specifically identify alginate.

2.9. Exoenzyme Assays

2.9.1. Protease Activity

Protease production was assessed on skim-milk agar (10% skim milk in nutrient agar) [28]. Standardized inocula were spotted onto plates and incubated at 37 °C for 24 h. Proteolytic activity was indicated by clear zones of casein hydrolysis surrounding colonies. Zone diameters were measured in millimeters and recorded for each isolate.

2.9.2. Lecithinase and Coagulase Activity

Lecithinase activity was evaluated on egg-yolk agar. After 24 h of incubation at 37 °C, the presence of an opaque precipitation zone surrounding colonies was recorded as lecithinase positive [29]. Coagulase production was tested by both slide and tube methods using citrated rabbit plasma. For the slide test, one to two colonies were emulsified in a drop of normal saline on a clean glass slide. A drop of citrated rabbit plasma was added to the suspension and mixed gently; visible clumping within 5–10 s was interpreted as positive (bound coagulase). All slide-negative results were confirmed by the tube test, in which citrated rabbit plasma was diluted 1:10 in physiological saline (0.2 mL plasma + 1.8 mL saline). Three labeled tubes test (T), positive control (*Staphylococcus aureus*), and negative control (sterile broth) each received 0.5 mL of diluted plasma. The test tube was inoculated with 0.1 mL of an 18–24-h broth culture and incubated at 37 °C; tubes were examined every 30 min for up to 4 h, and a final reading was taken at 24 h. Formation of a fibrin clot of any

size was recorded as positive (free coagulase); absence of clot formation was recorded as negative [30].

2.9.3. Hemolysin Production

A. Hemolysis on Blood Agar—Blood agar medium was prepared according to the manufacturer's instructions and sterilized by autoclaving. After the medium cooled to 45–50 °C, 5% human blood obtained from the hospital blood bank was added aseptically. Human blood was used because it was readily available through the hospital blood bank, whereas sheep blood was not readily accessible locally. The bacterial isolates were streaked onto the blood agar plates and incubated at 37 °C for 24 h. β-Hemolytic activity was assessed by observing the presence of a clear zone surrounding bacterial growth.

B. Cell-Free Hemolysin Assay—Cell-free hemolytic activity was assessed using the method described by Ridder et al. [30], with modifications. Briefly, 1.5 mL of a 2% suspension of washed human erythrocytes was mixed with 1.5 mL of cell-free bacterial supernatant obtained from planktonic cultures at a 1:1 (v/v) ratio. Human blood was obtained from the hospital blood bank. A negative control was prepared by mixing 1.5 mL of the same erythrocyte suspension with 1.5 mL of sterile culture medium without bacterial supernatant. A positive control representing complete erythrocyte lysis was included. The mixtures were incubated at 37 °C for 2 h and subsequently centrifuged at 5000× g for 5 min. The absorbance of the resulting supernatants was measured at 545 nm using a microplate spectrophotometer.

Hemolytic activity was expressed as a percentage and calculated using the following equation [31].

$$\text{HemolyticActivity}(\%) = \frac{A\text{sample} - A\text{ negative}}{\text{A positive} - \text{A negative}} \times 100$$

where A_sample is the absorbance of erythrocytes mixed with cell-free bacterial supernatant, A_negative is the absorbance of erythrocytes mixed with sterile culture medium, and A_positive is the absorbance corresponding to complete erythrocyte lysis.

2.9.4. Pyocin Production

The agar well diffusion method (Fyfe et al., 1984) [32] was applied for the estimation of pyocin production, but with slight modifications. Nutrient broth containing a 0.5 McFarland standard of a susceptible *S. aureus* indicator strain was allowed to incubate for 18 h at 37 °C. These were then spread uniformly across Mueller–Hinton agar plates.

Isolates were grown in nutrient broth for 24 h at 37 °C and were centrifuged at 10,000× g for 15 min. Supernatants were then filtered to sterilize using 0.22 µm membrane filters. Wells were prepared in the agar plates, and 100 µL aliquots of the filtered supernatants were added. Plates were incubated at 37 °C for 24 h, and diameters of inhibition zones were determined. Each experiment was performed in triplicate.

2.9.5. Pigment Production

Pyocyanin and pyoverdine production were assessed by culturing isolates on cetrimide agar and visually inspecting pigment formation after incubation at 37 °C. Pyocyanin was identified by its characteristic blue-green colour, whereas pyoverdine was recorded as a yellow-green fluorescent pigment. Results were recorded qualitatively as positive or negative for each isolate [33,34].

2.10. Adhesion to Human Uroepithelial Cells

The adhesion assay was based on a published epithelial-cell adherence method [35], with modifications described by Reid and Sobel [36].

Bacterial cells were centrifuged for 10 min at 10,000 rpm, 4 °C, and washed three times with phosphate-buffered saline (PBS, pH 7.2). The bacterial suspension was diluted and adjusted to 1×10^8 CFU/mL. Uroepithelial cells were isolated from pooled morning urine samples from four healthy female volunteers. The urine samples were pelleted by centrifuging 10 mL of urine at 5000 rpm for 10 min, then examined under a microscope by streaking one drop on a microscope slide and evaluating the presence of epithelial cells in the samples. After staining with 0.01% Trypan blue, cells were washed three times with PBS (pH 7.2) and counted in a Neubauer chamber. Viable uroepithelial cells were diluted to 1×10^5 cells/mL. An equal volume (1 mL) of each suspension (bacterial and uroepithelial cells) was mixed and incubated for 1 h at 37 °C. The smears were air-dried, fixed with methanol, and stained with Giemsa stain. Bacteria adhering to 30 uroepithelial cells were counted microscopically, and the average number of adhering bacteria per cell was calculated. Each experiment was performed in triplicate.

2.11. PCR Detection of Virulence and Resistance-Associated Genes

Genomic DNA extracted as described above was used as a template for PCR amplification of four target genes. All target genes were amplified using the same PCR cycling program, consisting of 30 cycles of denaturation at 94 °C for 1 min, annealing at 60 °C for 1 min, and extension at 72 °C for 1 min. The primer sequences, expected amplicon sizes, and PCR cycling conditions are summarized in Table 1. PCR products were separated by electrophoresis on a 1.2% agarose gel containing ethidium bromide and visualized under UV transillumination. Amplicons of the expected sizes were interpreted as positive, and the presence or absence of each target gene was recorded for all isolates [37].

Table 1. PCR primers and amplification conditions used for detection of virulence and resistance-associated genes.

Gene	Function	Forward Primer (5′→3′) Reverse Primer (5′→3)		
16S rRNA	Species confirmation	GTGCCAGCAGCCGCGCTAA AGACCCGGGAACGTATTCAC	450	[38,39]
algD	Alginate biosynthesis	TTCCCTCGCAGAGAAAACATC CCTGGTTGATCAGGTCGATCT	520	[40]
lasR	Las quorum-sensing regulator	CGGGTATCGTACTAGGTGCATCA GACGGGAAAGCCAGGAAACTT	1100	[41]
oprD	Carbapenem outer-membrane porin	TCCGCAGGTAGCACTCAGTTC AAGCCGGATTCATAGGTGGTG	191	[42]
mexB	MexAB–OprM efflux pump transporter	GCCATTCTCATCGTGGAGTT GAACAGCGGTACCCAGAAGA	249	[24]

PCR cycling conditions: All target genes were amplified using the same program: 30 cycles of denaturation at 94 °C for 1 min, annealing at 60 °C for 1 min, and extension at 72 °C for 1 min.

2.12. Retrospective Epidemiological Survey

A retrospective epidemiological study was conducted by reviewing the bacteriology unit registry of Al-Ramadi Teaching Hospital, Ramadi, Anbar Governorate, Iraq, for the year 2025. All urine culture records were extracted, including date of collection, patient gender, hospital ward, VITEK 2 microbiological identification result, and antibiotic susceptibility

profiles. Patient names were replaced with anonymous numerical identifiers (UTI-001 to UTI-188) to ensure confidentiality. A total of 188 urine specimens were included. Culture results, bacterial species distribution, and antibiotic resistance and sensitivity patterns were analyzed descriptively.

2.13. Statistical Analysis

Data were entered into Microsoft Excel and analyzed using GraphPad Prism (version 8.4; GraphPad Software, San Diego, CA, USA). Quantitative measurements are summarized as mean ± standard deviation (SD) from three independent replicates. Differences in inhibition-zone diameters across the eight antimicrobial disks were assessed using the Friedman test followed by pairwise Wilcoxon signed-rank tests with Holm correction for multiple comparisons. Hemolysis measurements were compared using one-way ANOVA followed by Tukey's multiple-comparisons test. Adhesion categories were assigned descriptively using predefined thresholds; no inferential comparison was made between categories derived from the same adhesion index. A p-value < 0.05 was considered statistically significant.

3. Results

3.1. Isolation, Identification, and Confirmation of P. aeruginosa Urinary Isolates

Of the 100 urine samples processed, 20 isolates (20%) were identified as *P. aeruginosa* based on colony morphology, Gram-negative rod morphology, motility, oxidase and catalase positivity, and the characteristic biochemical profile. VITEK® 2 assigned high-confidence identification as *P. aeruginosa* to all 20 isolates, designated PA1–PA20. All 20 isolates yielded the expected approximately 450 bp 16S rRNA gene PCR amplicon. Sanger sequencing and phylogenetic analysis were performed on four selected isolates (labelled S1, S4, S6, and S14 in the sequence dataset), which clustered with reference *P. aeruginosa* sequences (Figure 1).

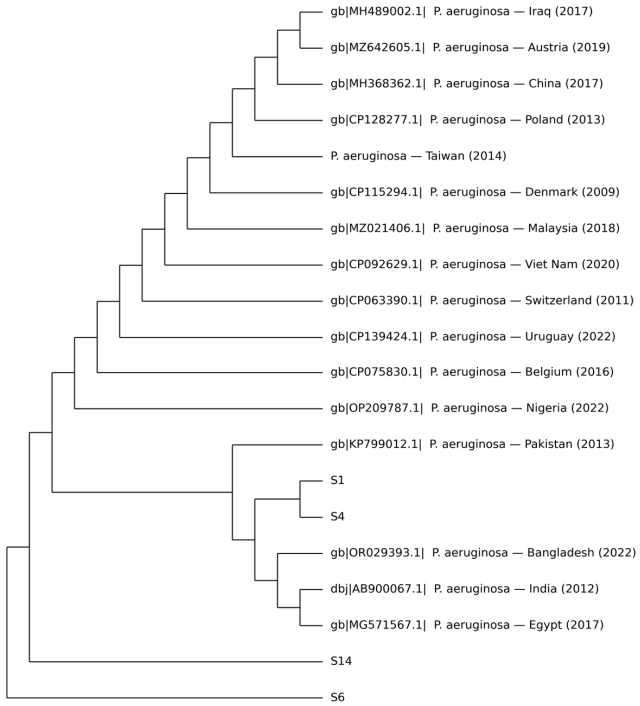


Figure 1. Phylogenetic relationships among four selected clinical isolates labelled S1, S4, S6, and S14 in the sequencing dataset and reference sequences obtained from GenBank. The tree was constructed using the Neighbor-Joining method with 1000 bootstrap replicates. Sequence-based phylogenetic analysis was performed on this selected subset; all 20 isolates were assessed by 16S rRNA gene PCR.

Additional identification documentation, including biochemical characterization, colony morphology, Gram staining, and motility findings, is provided in Supplementary Table S1 and Figures S1 and S2.

3.2. Antimicrobial Susceptibility Profile and MDR Status

Antimicrobial susceptibility testing of the 20 urinary *P. aeruginosa* clinical isolates revealed a substantial burden of antimicrobial resistance (Figure 2 and Table 2). Using the applicable CLSI M100-Ed35 interpretive criteria, resistance was observed in 90% of isolates to amikacin (AK), 45% to aztreonam (ATM), 85% to piperacillin (PRL), 80% to imipenem (IPM), 95% to ciprofloxacin (CIP), and 100% to ceftazidime (CAZ) and netilmicin (NET). For aztreonam, 35% of isolates were intermediate and 20% susceptible; for piperacillin, 10% were intermediate and 5% susceptible; for imipenem, 5% were intermediate and 15% susceptible; and for ciprofloxacin, 5% were intermediate. The remaining isolates in these categories were resistant. No isolates were susceptible to ciprofloxacin or ceftazidime. Gentamicin (CN) zone diameters are shown, but S/I/R categories were not assigned because CLSI M100-Ed35 does not provide disk-diffusion interpretive breakpoints for *P. aeruginosa*.

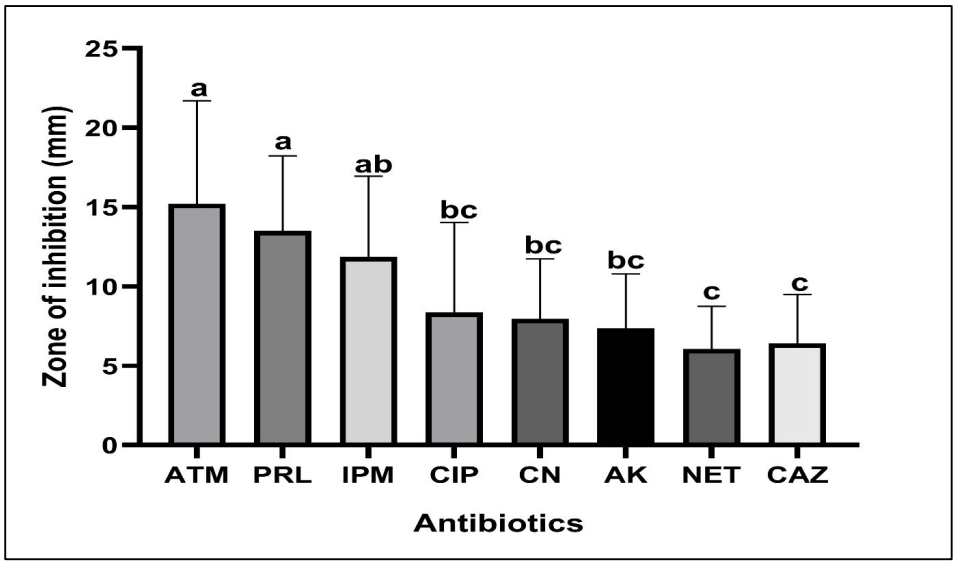


Figure 2. Mean inhibition-zone diameters (mm) of eight antibiotic disks tested against 20 urinary *Pseudomonas aeruginosa* clinical isolates using the Kirby–Bauer disk diffusion method. Bars represent the mean ± standard deviation (SD). Differences among antibiotics were assessed using the Friedman test, followed by pairwise Wilcoxon signed-rank tests with Holm correction for multiple comparisons. Where indicated, different lowercase letters denote statistically significant differences between groups (adjusted $p < 0.05$).

The multiple antibiotic resistance (MAR) index was calculated for each isolate using six antimicrobial agents: amikacin (AK), aztreonam (ATM), piperacillin (PRL), imipenem (IPM), ciprofloxacin (CIP), and ceftazidime (CAZ). The index was calculated as MAR = $a/6$, where a represents the number of these six agents to which an isolate was classified as resistant. Intermediate results were not counted as resistant. Across all 20 isolates, MAR indices ranged from 0.33 to 1.00, with a mean of 0.825 (approximately 0.83). Fifteen isolates (75%) had MAR indices ≥0.80, and seven isolates (35%) had a MAR index of 1.00. PA3 had the lowest MAR index (0.33), whereas PA4, PA8, PA13, PA15, PA16, PA17, and PA20 had an MAR index of 1.00. PA19 had an MAR index of 0.83.

Table 2. Antibiotic Susceptibility Profiles and MAR Indices of 20 Urinary *Pseudomonas aeruginosa* Clinical Isolates.

Isolate	AK	ATM	PRL	IPM	CN	CIP	NET	CAZ	MAR (a/6)
PA1	10 (R)	20 (I)	11 (R)	7 (R)	10 (NI)	18 (R)	8 (R)	8 (R)	0.83
PA2	9 (R)	19 (I)	15 (R)	10 (R)	11 (NI)	14 (R)	9 (R)	9 (R)	0.83
PA3	17 (S)	23 (S)	16 (R)	24 (S)	14 (NI)	24 (I)	7 (R)	8 (R)	0.33
PA4	10 (R)	9 (R)	6 (R)	9 (R)	9 (NI)	11 (R)	8 (R)	7 (R)	1.00
PA5	8 (R)	25 (S)	15 (R)	23 (S)	11 (NI)	6 (R)	9 (R)	9 (R)	0.67
PA6	14 (R)	20 (I)	9 (R)	9 (R)	6 (NI)	6 (R)	7 (R)	7 (R)	0.83
PA7	19 (S)	20 (I)	25 (S)	11 (R)	7 (NI)	9 (R)	8 (R)	9 (R)	0.50
PA8	9 (R)	8 (R)	14 (R)	9 (R)	19 (NI)	9 (R)	7 (R)	8 (R)	1.00
PA9	9 (R)	18 (I)	11 (R)	9 (R)	10 (NI)	8 (R)	9 (R)	8 (R)	0.83
PA10	6 (R)	22 (S)	12 (R)	10 (R)	6 (NI)	11 (R)	8 (R)	6 (R)	0.83
PA11	8 (R)	20 (I)	16 (R)	20 (S)	6 (NI)	7 (R)	10 (R)	6 (R)	0.67
PA12	9 (R)	22 (S)	16 (R)	8 (R)	6 (NI)	10 (R)	6 (R)	6 (R)	0.83
PA13	11 (R)	8 (R)	7 (R)	11 (R)	8 (NI)	11 (R)	8 (R)	9 (R)	1.00
PA14	7 (R)	18 (I)	9 (R)	9 (R)	9 (NI)	12 (R)	6 (R)	10 (R)	0.83
PA15	8 (R)	6 (R)	7 (R)	7 (R)	6 (NI)	10 (R)	8 (R)	7 (R)	1.00
PA16	8 (R)	9 (R)	12 (R)	7 (R)	6 (NI)	8 (R)	9 (R)	7 (R)	1.00
PA17	9 (R)	11 (R)	15 (R)	13 (R)	6 (NI)	9 (R)	11 (R)	9 (R)	1.00
PA18	9 (R)	6 (R)	18 (I)	16 (I)	9 (NI)	8 (R)	8 (R)	10 (R)	0.67
PA19	9 (R)	12 (R)	20 (I)	12 (R)	6 (NI)	9 (R)	7 (R)	11 (R)	0.83
PA20	7 (R)	8 (R)	16 (R)	13 (R)	8 (NI)	10 (R)	9 (R)	12 (R)	1.00

Note: Values are inhibition-zone diameters (mm), followed by the susceptibility interpretation in parentheses: S, susceptible; I, intermediate; R, resistant. NI indicates that no S/I/R category was assigned because CLSI M100-Ed35 (2025) does not provide disk-diffusion interpretive breakpoints for gentamicin against *P. aeruginosa*. AK, amikacin; ATM, aztreonam; PRL, piperacillin; IPM, imipenem; CN, gentamicin; CIP, ciprofloxacin; NET, netilmicin; CAZ, ceftazidime. The MAR index was calculated as a/6, where a is the number of resistant results among AK, ATM, PRL, IPM, CIP, and CAZ; intermediate results were not counted as resistant. Netilmicin was interpreted using the applicable CLSI M100-Ed35 criteria but was excluded from the MAR calculation.

Multidrug resistance (MDR) was defined as non-susceptibility to at least one antimicrobial agent in three or more antimicrobial categories, in accordance with the consensus definition proposed by Magiorakos et al. [23]. Both resistant and intermediate results were considered non-susceptible for this classification. Based on the susceptibility results in Table 2, all 20 isolates (100%) met the MDR criterion. PA3 also met this criterion because it was resistant to piperacillin and ceftazidime and showed intermediate susceptibility to ciprofloxacin, representing non-susceptibility across three antimicrobial categories.

Inhibition-zone diameters differed significantly among the eight tested antimicrobial disks, according to the Friedman test ($\chi^2(7) = 35.13$, $p < 0.001$). The largest mean inhibition-zone diameters were observed for ATM (15.20 ± 6.49 mm) and PRL (13.50 ± 4.73 mm), whereas the smallest were observed for NET (8.00 ± 1.26 mm) and CAZ (8.30 ± 1.66 mm). Pairwise Wilcoxon signed-rank tests with Holm correction identified significant differences between PRL and NET (adjusted $p = 0.007$), PRL and CAZ (adjusted $p = 0.010$), IPM and CAZ (adjusted $p = 0.017$), IPM and NET (adjusted $p = 0.021$), and ATM and NET (adjusted $p = 0.033$). These comparisons indicate differences in measured inhibition-zone diameters and should not be interpreted as direct evidence of comparative clinical efficacy.

3.3. Biofilm-Forming Ability

All 20 urinary *P. aeruginosa* clinical isolates demonstrated biofilm-forming capacity across all three assay methods, with varying intensities (Table 3). No isolate was classified as a non-biofilm producer by any method.

Table 3. Biofilm formation by 20 urinary *P. aeruginosa* isolates and the ATCC 15442 reference strain, assessed using three complementary methods.

Isolate	CV (Mean ± SD)	Biofilm	Tube Assay	CRA Method
PA1	0.3940 ± 0.0111	Strong	+++	Black Crystalline
PA2	0.2250 ± 0.0259	Moderate	++	Black Crystalline
PA3	0.2767 ± 0.0432	Moderate	++	Black Crystalline
PA4	0.4433 ± 0.0155	Strong	+++	Black Crystalline
PA5	0.2970 ± 0.0204	Moderate	+++	Black Crystalline
PA6	0.4337 ± 0.0076	Strong	+++	Black Crystalline
PA7	0.3100 ± 0.0471	Moderate	+++	Black Crystalline
PA8	0.2823 ± 0.0180	Moderate	+++	Black Crystalline
PA9	0.2270 ± 0.0299	Moderate	+	Black Crystalline
PA10	0.2713 ± 0.0200	Moderate	++	Black Crystalline
PA11	0.2827 ± 0.0225	Moderate	+++	Black Crystalline
PA12	0.2393 ± 0.0144	Moderate	+	Black Crystalline
PA13	0.2900 ± 0.0382	Moderate	++	Black Crystalline
PA14	0.4460 ± 0.0312	Strong	+++	Black Crystalline
PA15	0.2533 ± 0.0236	Moderate	++	Black Crystalline
PA16	0.3033 ± 0.0108	Moderate	+++	Black Crystalline
PA17	0.2767 ± 0.0051	Moderate	++	Black Crystalline
PA18	0.2333 ± 0.0068	Moderate	++	Black Crystalline
PA19	0.2700 ± 0.0182	Moderate	++	Black Crystalline
PA20	0.2100 ± 0.0085	Moderate	+	Black Crystalline
ATCC 15442	0.1713 ± 0.0095	Weak	—	pink

Note: CV = crystal violet microtiter plate assay. ODc = 0.0900 (mean of negative controls 0.0600 + 3 × SD 0.0100). Biofilm categories [25]: Non-biofilm (OD ≤ 0.0900); Weak (0.0900 < OD ≤ 0.1800); Moderate (0.1800 < OD ≤ 0.3600); Strong (OD > 0.3600). Tube assay: (+) weak; (++) moderate; (+++) strong. CRA: black/dry colony = biofilm producer; pink/red = weak/non-producer. ATCC 15442 was used as the reference control strain.

In the CV microtiter plate assay (ODc = 0.0900), 4 isolates (20%) were classified as strong biofilm producers: PA1 (0.3940 ± 0.0111), PA4 (0.4433 ± 0.0155), PA6 (0.4337 ± 0.0076), and PA14 (0.4460 ± 0.0312), with mean OD_{570} values exceeding the 4 × ODc threshold of 0.3600. The remaining 16 isolates (80%) were classified as moderate biofilm producers, with mean OD_{570} values ranging from 0.2100 ± 0.0085 (PA20) to 0.3100 ± 0.0471 (PA7), all falling within the 2 × ODc–4 × ODc range (0.1800–0.3600). The reference strain *P. aeruginosa* ATCC 15442 yielded a mean OD_{570} of 0.1713 ± 0.0095, classified as a weak biofilm producer, confirming the validity and reliability of the assay conditions.

In the tube adherence assay, strong biofilm formation (+++) was observed in PA1, PA4, PA5, PA6, PA7, PA8, PA11, PA14, PA16 (9 isolates; 45%), moderate formation (++) in PA2, PA3, PA10, PA13, PA15, PA17, PA18, PA19 (8 isolates; 40%), and weak formation (+) in PA9,

PA12, and PA20 (3 isolates; 15%). By the Congo Red Agar (CRA) method, all 20 clinical isolates produced black crystalline colonies, consistent with strong exopolysaccharide-mediated biofilm production, while ATCC 15442 produced pink colonies, indicative of weak or absent biofilm formation. Overall concordance across the three methods was high, with all 20 isolates (100%) confirmed as biofilm producers. Strong and moderate producers constituted 100% of clinical isolates by the quantitative CV assay, and the qualitative tube adherence and CRA methods were largely consistent with these findings. The strong-to-moderate biofilm-forming phenotype observed across all isolates, combined with their MDR profile, underscores the significant clinical challenge posed by these urinary *P. aeruginosa* strains, as biofilm formation is a well-established mechanism of antibiotic tolerance and treatment failure.

3.4. Pyocin Production

All 20 clinical *P. aeruginosa* isolates produced pyocin activity, although inhibition-zone diameters varied substantially (Table 4). Inhibition zones against the *S. aureus* ATCC 25923 indicator strain ranged from 5.03 ± 1.72 mm (PA12) to 25.03 ± 0.25 mm (PA1). Five isolates (PA1, PA4, PA9, PA14, and PA19) were classified as strong producers (>20 mm), three (PA2, PA11, and PA12) showed weak activity (<10 mm), and the remaining 12 showed moderate activity (10–20 mm).

Table 4. Pyocin production by urinary *P. aeruginosa* isolates, determined by the well-diffusion method against *Staphylococcus aureus* ATCC 25923.

Isolate	Inhibition Zone (mm) Mean ± SD	Activity Classification
PA1	25.03 ± 0.25	Strong
PA2	8.67 ± 1.53	Weak
PA3	10.67 ± 1.53	Moderate
PA4	21.50 ± 1.18	Strong
PA5	13.80 ± 0.30	Moderate
PA6	10.50 ± 0.30	Moderate
PA7	13.80 ± 0.30	Moderate
PA8	11.73 ± 0.95	Moderate
PA9	21.87 ± 1.42	Strong
PA10	15.30 ± 0.89	Moderate
PA11	6.50 ± 1.18	Weak
PA12	5.03 ± 1.72	Weak
PA13	17.03 ± 1.54	Moderate
PA14	22.80 ± 0.30	Strong
PA15	18.97 ± 0.25	Moderate
PA16	12.83 ± 0.65	Moderate
PA17	13.80 ± 0.30	Moderate
PA18	10.50 ± 0.30	Moderate
PA19	20.47 ± 0.35	Strong
PA20	19.40 ± 1.25	Moderate
ATCC 15442	3.04 ± 1.78	Weak

Note: Values represent mean ± SD from three independent replicates. Activity classification: weak (<10 mm), moderate (10–20 mm), and strong (>20 mm).

Representative agar plates showing pyocin production and inhibition-zone measurements for the clinical isolates are presented in Supplementary Figures S4 and S5.

3.5. Capsule-Associated Extracellular Polysaccharide and Exoenzyme Activity

Phenotypic testing indicated capsule-associated extracellular polysaccharide production in all 20 clinical isolates and the ATCC 15442 reference strain (Table 5). Because India ink reveals capsule-associated material generally, this result should not be interpreted as alginate-specific detection. Protease activity was detected in all 20 clinical isolates, as indicated by clear casein-hydrolysis zones on skim-milk agar. Lecithinase and coagulase activity were not detected under the assay conditions used (Table 5); these negative results should not be interpreted as evidence that the factors are universally absent or irrelevant to uropathogenicity. Representative images of the phenotypic assays are provided in Supplementary Figure S3.

Table 5. Virulence phenotype profile of urinary *P. aeruginosa* isolates (PA1–PA20) and ATCC 15442 reference strain.

Isolates	Capsules	Protease	Lecithinase	Coagulase	β-Hemolysis	Pyocyanin	Pyoverdine
PA1	+	+	−	−	+	+	+
PA2	+	+	−	−	+	+	−
PA3	+	+	−	−	+	+	−
PA4	+	+	−	−	+	−	−
PA5	+	+	−	−	+	+	+
PA6	+	+	−	−	+	+	−
PA7	+	+	−	−	+	+	+
PA8	+	+	−	−	+	+	−
PA9	+	+	−	−	+	+	−
PA10	+	+	−	−	+	−	+
PA11	+	+	−	−	+	+	−
PA12	+	+	−	−	+	−	−
PA13	+	+	−	−	+	+	−
PA14	+	+	−	−	+	+	+
PA15	+	+	−	−	+	+	−
PA16	+	+	−	−	+	−	−
PA17	+	+	−	−	+	+	+
PA18	+	+	−	−	+	+	−
PA19	+	+	−	−	+	+	−
PA20	+	+	−	−	+	+	+
ATCC 15442	+	+	−	−	+	+	+

Note: (+) = positive; (−) = negative.

3.6. Hemolysin Production

All 20 isolates exhibited β-hemolysis on blood agar. Quantitative cell-free hemolysis ranged from 2.20 ± 0.20% (PA20) to 13.20 ± 7.30% (PA6), with most isolates showing values below 10% (Figure 3). PA3, PA6, PA7, PA9, PA10, and PA15 showed comparatively higher hemolysis values than the other clinical isolates. The ATCC 15442 reference strain showed minimal hemolysis (0.87 ± 0.64%). One-way ANOVA followed by Tukey's multiple-

comparisons test identified PA6 as significantly higher than the reference strain ($p < 0.001$). These results describe erythrocyte lysis under the assay conditions and should not be interpreted as direct measures of clinical severity.

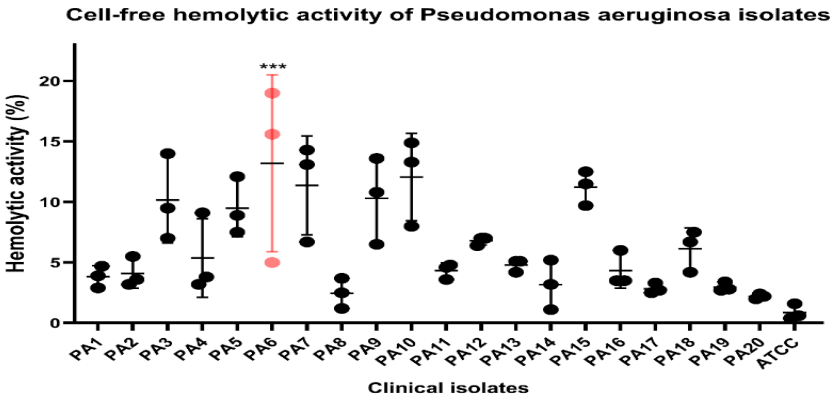


Figure 3. Cell-free hemolytic activity of *P. aeruginosa* clinical isolates. Data are shown as individual replicates with mean ± standard deviation. One-way ANOVA followed by Tukey's multiple-comparisons test identified significantly higher hemolytic activity for PA6 than for the ATCC reference strain (*** $p < 0.001$).

3.7. Pigment Production and Adhesion to Uroepithelial Cells

Pyocyanin was detected in 16 of 20 clinical isolates (80%), whereas pyoverdine was detected in seven of 20 isolates (35%), consistent with the isolate-level results in Table 5. The pigments were identified by their characteristic colour or fluorescence as described in the Methods.

Adhesion to human uroepithelial cells varied among isolates (Table 6, Figure 4). Adhesion indices ranged from 4.3 to 19.5 bacteria per cell, with an overall mean of 11.4 ± 5.1 bacteria per cell. Based on the predefined thresholds, 11 isolates (55%) were classified as high-adherence (>10 bacteria/cell), seven (35%) as moderate (5–10 bacteria/cell), and two (10%) as low-adherence (<5 bacteria/cell). These categories are descriptive classifications derived from the same adhesion index and were not compared using an inferential statistical test.

Table 6. Adhesion index and adhesion category of urinary *P. aeruginosa* isolates and ATCC 15442 reference strain.

Isolate	Adhesion Index (Bacteria/Cell)	Adhesion Category
PA1	6.2 ± 0.5	Moderate
PA2	12.5 ± 0.8	High
PA3	8.1 ± 0.6	Moderate
PA4	4.3 ± 0.4	Low
PA5	15.2 ± 1.1	High
PA6	18.4 ± 1.3	High
PA7	13.6 ± 0.9	High
PA8	7.5 ± 0.5	Moderate
PA9	10.2 ± 0.7	High
PA10	14.1 ± 0.8	High
PA11	6.8 ± 0.6	Moderate
PA12	9.3 ± 0.7	Moderate

Table 6. *Cont.*

Isolate	Adhesion Index (Bacteria/Cell)	Adhesion Category
PA13	16.7 ± 1.2	High
PA14	19.5 ± 1.4	High
PA15	5.6 ± 0.4	Moderate
PA16	11.8 ± 0.9	High
PA17	7.2 ± 0.5	Moderate
PA18	4.8 ± 0.3	Low
PA19	17.9 ± 1.2	High
PA20	18.8 ± 1.3	High
ATCC 15442	6.2 ± 0.5	Moderate

Adhesion categories: low (<5 bacteria/cell), moderate (5–10 bacteria/cell), and high (>10 bacteria/cell). Values represent mean ± SD from three replicates.

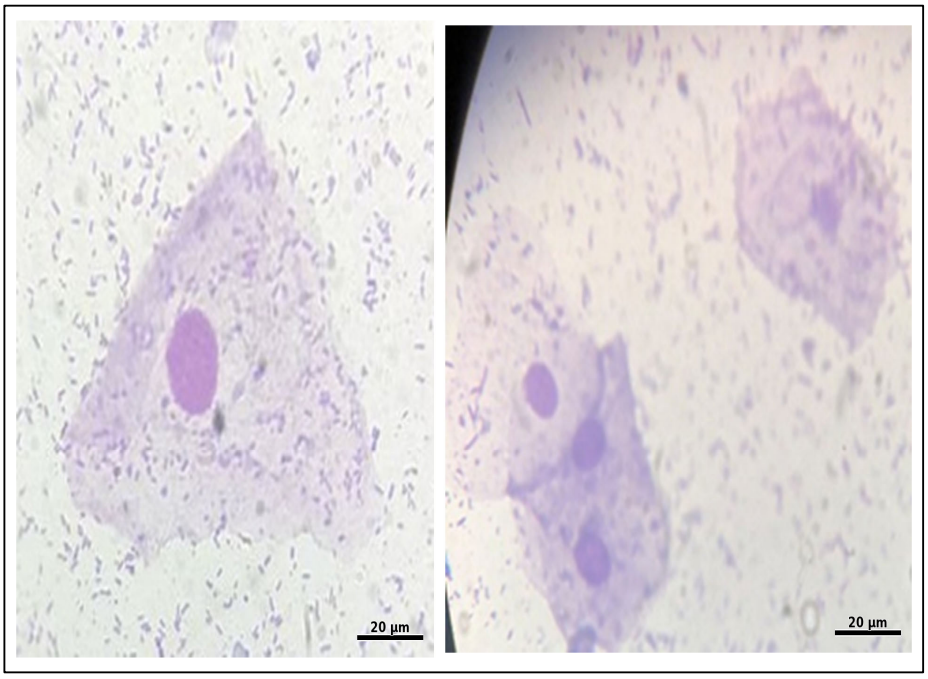


Figure 4. Representative micrographs of *P. aeruginosa* adhering to human uroepithelial cells. Quantitative adhesion indices for the individual isolates are provided in Table 6.

3.8. Detection of Virulence and Resistance-Associated Genes

PCR amplification of the four target regions, *algD*, *lasR*, *oprD*, and *mexB*, was performed on genomic DNA from all 20 urinary *P. aeruginosa* isolates (PA1–PA20), with *P. aeruginosa* ATCC 15442 as a positive control. Representative gel images of four selected isolates are shown in Figure 5.

The *algD* target, associated with alginate biosynthesis, was detected in all 20 isolates (100%) and produced the expected amplicon of approximately 520 bp. This establishes the presence of the targeted DNA region but does not demonstrate *algD* expression or alginate production. The India ink results indicate capsule-associated extracellular polysaccharide, which is not specific to alginate.

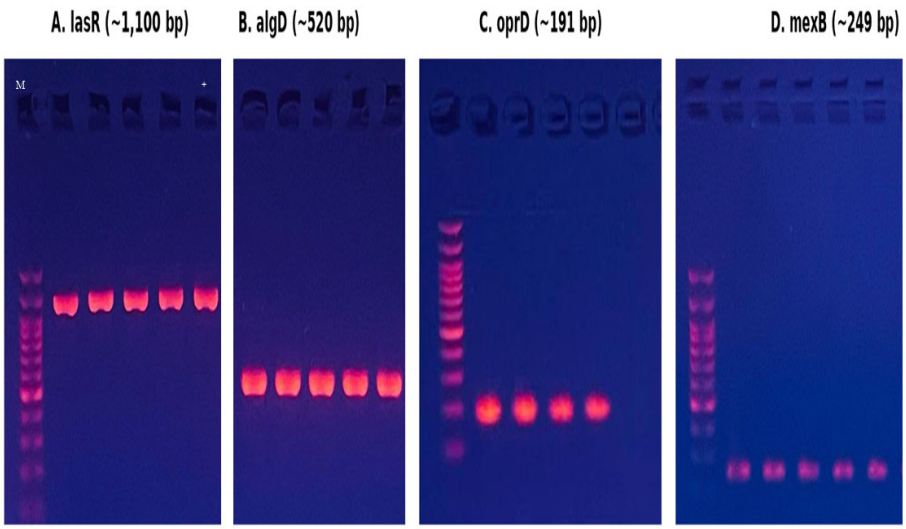


Figure 5. Representative PCR amplification of *algD*, *lasR*, *oprD*, and *mexB* in four selected *P. aeruginosa* isolates (PA1, PA4, PA6, and PA14). Panel (**A**): *lasR* (~1100 bp); panel (**B**): *algD* (~520 bp); panel (**C**): *oprD* (~191 bp); and panel (**D**): *mexB* (~249 bp). Lane M represents the 100-bp DNA ladder; lanes 2–5 represent PA1, PA4, PA6, and PA14, respectively, and lane (+) represents *P. aeruginosa* ATCC 15442 as the positive control. the figure shows representative gel examples; all 20 isolates were tested and were positive for all four target regions. The 16S rRNA gene sequences for the sequenced isolates were deposited in GenBank under accession numbers PV014006 (PA1), PV014007 (PA4), PV014008 (PA6), and PV014009 (PA14) (submission ID: SUB15032956).

The *lasR* target was detected in all 20 isolates (100%), producing the expected amplicon of approximately 1100 bp. This confirms the presence of the targeted region but does not establish that *lasR* is intact, expressed, or functionally regulates quorum-sensing pathways.

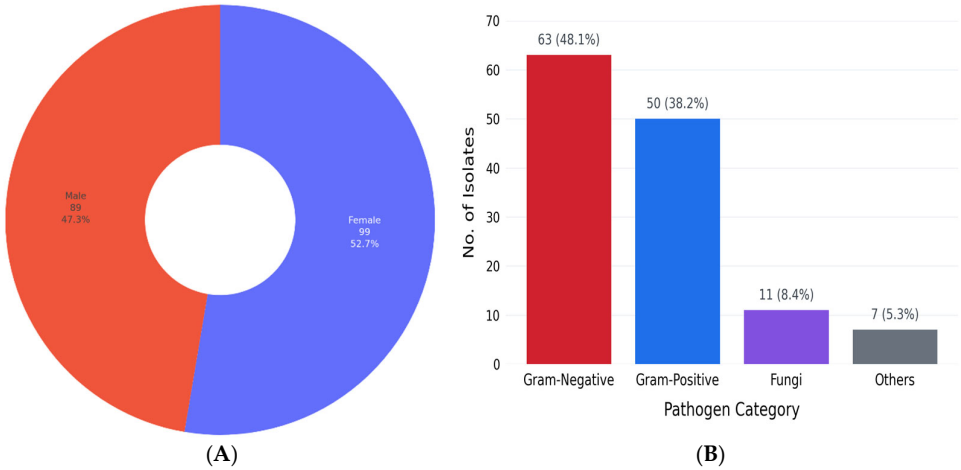
The *oprD* target was detected in all 20 isolates (100%), with an expected amplicon of 191 bp. Detection of this region does not exclude sequence changes elsewhere in *oprD* or reduced expression, and it cannot establish the mechanism underlying the observed imipenem resistance.

The *mexB* target was detected in all 20 isolates (100%), with an expected amplicon of 249 bp. Its presence is consistent with the genetic potential for the MexAB–OprM efflux system but does not establish overexpression or causation of resistance to any specific antibiotic. Chloramphenicol was not included in the susceptibility panel, so no chloramphenicol-resistance conclusion is drawn from this study.

Taken together, the phenotypic assays documented biofilm formation, capsule-associated extracellular polysaccharide, protease activity, β-hemolysis, pyocin activity, variable pigment production, and variable adhesion. PCR detected all four target regions in all 20 isolates. Because target detection was uniform, these data cannot establish associations between gene presence or absence and differences in resistance or virulence phenotypes. The findings demonstrate the coexistence of MDR and multiple virulence-associated traits in this cohort, not a causal relationship between individual genes and phenotypes.

3.9. Epidemiological Profile of UTI (2025)

A retrospective review of the Al-Ramadi Teaching Hospital bacteriology registry for 2025 identified 188 urine-culture records. Of these, 131 (69.7%) were culture-positive and 57 (30.3%) showed no growth. Female patients accounted for 52.7% of records ($n = 99$), compared with 47.3% for male patients ($n = 89$) (Figure 6).



(**A**) (**B**)

Figure 6. Retrospective epidemiological summary of the 2025 urine-culture records: (**A**) patient sex distribution among 188 records; (**B**) distribution of Gram-negative, Gram-positive, fungal, and other groups among the 131 culture-positive records.

Among the positive cultures, *Escherichia coli* was the most frequently identified uropathogen (27.5%, $n = 36$), followed by *Staphylococcus aureus* (26.0%, $n = 34$), *Klebsiella pneumoniae* (9.2%, $n = 12$), *Candida*/yeast (8.4%, $n = 11$), *Pseudomonas aeruginosa* (7.6%, $n = 10$), *Streptococcus* spp. (6.9%, $n = 9$), *Enterococcus faecalis* (3.8%, $n = 5$), and *Burkholderia* spp. (2.3%, $n = 3$). Additional organisms were classified under the "Others" category, as presented in Table 7.

Table 7. Bacterial species recovered from 188 urine culture records reviewed retrospectively at Al-Ramadi Teaching Hospital, Ramadi, Iraq, in 2025.

Rank	Organism	No. of Isolates	% of Positives
1	*Escherichia coli*	36	27.5%
2	*Staphylococcus aureus*	34	26.0%
3	*Klebsiella pneumoniae*	12	9.2%
4	*Candida*/Yeast	11	8.4%
5	*Pseudomonas aeruginosa*	10	7.6%
6	*Streptococcus* spp.	9	6.9%
7	*Enterococcus faecalis*	5	3.8%
8	*Burkholderia* spp.	3	2.3%
9	Others	11	8.4%

Note: *E. coli* was the most frequently identified uropathogen (27.5%), followed by *S. aureus* (26.0%); *K. pneumoniae* ranked third (9.2%). Two *E. coli* isolates were reported as ESBL-producing based on VITEK 2 MIC data, and two *P. aeruginosa* isolates were recorded as pan-drug-resistant in the urology ward. These findings describe the hospital records reviewed in this study and should not be generalized beyond the sampled population.

Regarding antibiotic resistance, ciprofloxacin exhibited the highest resistance frequency ($n = 40$, 30.5%), followed by gentamicin ($n = 33$, 25.2%), ceftriaxone ($n = 23$, 17.6%), ampicillin ($n = 21$, 16.0%), and trimethoprim/sulfamethoxazole ($n = 21$, 16.0%). Conversely, amikacin demonstrated the highest sensitivity rate ($n = 58$, 44.3%), followed by gentamicin ($n = 49$, 37.4%), imipenem ($n = 43$, 32.8%), and nitrofurantoin ($n = 43$, 32.8%) (Table 8).

Table 8. Antibiotic Susceptibility Profiles of Bacterial Isolates Recovered from UTI Patients in 2025.

Antibiotic	Class	No. Resistant (R)	No. Sensitive (S)	Predominant Profile
ciprofloxacin	Fluoroquinolone	40	31	Resistant
gentamicin	Aminoglycoside	33	49	Mixed
amikacin	Aminoglycoside	17	58	Sensitive
tobramycin	Aminoglycoside	21	25	Mixed
imipenem	Carbapenem	—	43	Sensitive
meropenem	Carbapenem	—	24	Sensitive
ceftriaxone	3rd-gen Cephalosporin	23	—	Resistant
ceftazidime	3rd-gen Cephalosporin	16	28	Mixed
ampicillin	Penicillin	21	—	Resistant
piperacillin	Extended-spectrum Penicillin	18	—	Resistant
trimethoprim/sulfamethoxazole	Folate Inhibitor	21	—	Resistant
levofloxacin	Fluoroquinolone	16	24	Mixed
nitrofurantoin	Nitrofuran	—	43	Sensitive
erythromycin	Macrolide	18	—	Resistant
tetracycline	Tetracycline	18	—	Resistant
tigecycline	Glycylcycline	—	27	Sensitive

Note: values indicate the dominant phenotype. (—) indicates not prominently reported in the opposite category.

4. Discussion

This study characterized phenotypic virulence-associated traits and antimicrobial resistance in 20 *P. aeruginosa* isolates recovered from urine samples. Conventional biochemical tests and VITEK® 2 identified all 20 isolates as *P. aeruginosa*, and all yielded the expected 16S rRNA gene PCR amplicon. Sequence-based phylogenetic analysis was performed on four selected isolates, rather than on the entire collection. The 20% proportion observed in the laboratory component should therefore be interpreted in the context of its sample and sampling strategy, not as a hospital-wide prevalence estimate. In the separate 2025 retrospective cohort, *P. aeruginosa* accounted for 7.6% of positive urine cultures.

The main finding was the coexistence of multidrug resistance (MDR) and biofilm-forming capacity among the urinary *P. aeruginosa* isolates. All 20 isolates met the study's MDR criterion, and the MAR indices ranged from 0.33 to 1.00; 15 isolates (75%) had MAR indices ≥0.80. The Friedman test identified differences in inhibition-zone diameters among the eight tested antimicrobial disks ($\chi^2(7) = 35.13$, $p < 0.001$). The largest mean zones were observed for aztreonam and piperacillin, while the smallest were observed for netilmicin and ceftazidime. These measurements describe in-vitro inhibition-zone differences and do not establish comparative clinical efficacy. The underlying resistance mechanisms were not directly tested.

All 20 isolates had MAR indices above 0.20. This threshold has historically been used in source-tracking studies of antimicrobial-resistant *E. coli*, but it is not a validated clinical-outcome threshold for *P. aeruginosa*. Its interpretation in this clinical cohort should therefore be cautious [43].

The universal biofilm-forming capacity detected by the crystal violet, tube adherence, and Congo red agar methods supports the classification of all 20 clinical isolates as biofilm producers. In the quantitative crystal violet assay, four isolates (20%) were strong producers and 16 (80%) were moderate producers. Biofilms on urinary catheters and uroepithelial

surfaces can be difficult to eradicate and may contribute to persistence or recurrence of catheter-associated infections [1,4]. Detection of *algD* and *lasR* is biologically relevant to alginate biosynthesis and quorum-sensing regulation, respectively, but PCR positivity alone does not demonstrate transcription, protein production, or functional activity. Because all isolates carried the four targeted regions, their presence cannot explain the variation in biofilm intensity observed in this cohort. The coexistence of MDR and biofilm formation may complicate bacterial eradication, but these data do not establish a causal relationship between the traits.

The broad phenotypic profile included capsule-associated extracellular polysaccharide production, protease activity, and β-hemolysis in all clinical isolates, alongside variable pyocin activity intensity and pigment production. Lecithinase and coagulase activity were not detected under the assay conditions used; these negative findings do not establish that the factors are unimportant in other settings. Pyocyanin and pyoverdine are associated with oxidative stress and iron acquisition, respectively, but their clinical effects were not measured in this study. The strong pyocin activity observed in five isolates is of microbiological interest, although its contribution to competition within polymicrobial urinary infections was not evaluated.

Adhesion to uroepithelial cells, an early step in UTI pathogenesis, was high in 55% of isolates, with adhesion indices ranging from 4.3 to 19.5 bacteria per cell. Adhesion is important in urinary tract colonization, and variation in this phenotype may reflect differences in the expression or activity of surface-associated structures and regulatory pathways that were not measured directly in this study [1,35]. Together with biofilm formation, the observed adhesion phenotype is consistent with the potential for colonization and persistence on uroepithelial surfaces or urinary devices; however, the study did not directly assess catheter-associated outcomes.

The genotype–phenotype findings should be interpreted as complementary observations rather than proof of direct causation. PCR detected *algD*, *lasR*, *oprD*, and *mexB* target regions in all 20 isolates, whereas biofilm intensity and cellular adhesion varied. Thus, presence or absence of these targets did not explain the phenotypic variation in this cohort. Detection of *mexB* is consistent with the genetic potential for MexAB–OprM-mediated efflux, but it does not establish pump overexpression or its contribution to an individual isolate's resistance profile. Detection of an *oprD* amplicon confirms only the presence of the targeted DNA region; it does not exclude sequence changes elsewhere in the gene or reduced expression, and it cannot identify the mechanism responsible for imipenem resistance. As all isolates were positive for all four targets, presence/absence associations with MDR, biofilm intensity, or adhesion could not be tested. Future studies should combine gene sequencing, quantitative expression analysis, functional efflux or porin assays, and isolate-level correlation analyses.

The combined MDR and virulence-associated phenotype observed here is broadly consistent with reports from other settings [2,4]. This study adds a single-cohort description of urinary isolates by integrating antimicrobial susceptibility, biofilm assays, adhesion measurements, and selected virulence-associated phenotypes. The relatively small, single-centre sample should be considered when interpreting these findings.

From a clinical perspective, the coexistence of MDR, biofilm formation, and uroepithelial adhesion may complicate eradication of urinary *P. aeruginosa*, particularly in complicated or catheter-associated infections. These findings support susceptibility-guided antimicrobial selection, appropriate urinary-catheter management, and infection-prevention practices. However, the study did not link individual isolates' genotypes and phenotypes to patient-level data on symptom severity, catheter exposure, recurrence, comorbidities, or treatment response. The possible implications for persistence or treatment difficulty should therefore

be considered biologically plausible rather than demonstrated associations with clinical manifestations or patient outcomes.

Limitations include the small number of *P. aeruginosa* isolates (n = 20) from a single centre, which may limit generalizability. Sequence-based phylogenetic analysis was performed on only four selected isolates, and PCR detection was not accompanied by full-length sequencing, gene-expression measurements, or functional assays. Because *algD*, *lasR*, *oprD*, and *mexB* were detected in all isolates, the study could not test whether gene presence or absence was associated with variation in biofilm formation, adhesion, or resistance. The retrospective component lacked complete patient-level outcome information, including treatment response, recurrence, catheter exposure, and comorbidities. Human erythrocytes were used in the hemolysis assays because sheep blood was not readily available locally; this may limit direct comparability with studies using sheep erythrocytes. Future multicentre studies with larger cohorts, functional testing, and linked clinical outcomes are needed.

The retrospective survey included 188 urine-culture records, of which 131 (69.7%) were culture-positive. This was a descriptive hospital-record review, and the culture positivity rate should not be interpreted as a population-level prevalence estimate. The sex distribution was relatively balanced, with 99 female and 89 male records. The separate laboratory component involved 100 urine samples and 20 *P. aeruginosa* isolates; the denominators and findings of the two components should be interpreted independently.

E. coli was the most frequently identified organism in the retrospective survey, accounting for 27.5% of positive cultures. *P. aeruginosa* accounted for 7.6% of positive cultures, and two isolates from urology ward records were reported as pan-drug-resistant. Ciprofloxacin resistance was recorded in 30.5% of the positive-culture cohort, while trimethoprim/sulfamethoxazole resistance was recorded in 16.0%. Because these agents have been used empirically in some local settings, the findings support reviewing empirical-treatment protocols against current, institution-specific surveillance data. The highest recorded susceptibility proportions were for amikacin and imipenem (44.3% and 32.8%, respectively), but these proportions also indicate that susceptibility remained limited. Treatment decisions should therefore be guided by validated susceptibility results and the patient's clinical context.

Emerging rapid antimicrobial susceptibility testing (AST) technologies may be relevant to UTI management where resistance is common. Conventional culture and susceptibility workflows can delay targeted treatment, whereas selected rapid platforms have reported results within approximately 30 min to a few hours, depending on the technology, specimen, and workflow [44,45]. Molecular–phenotypic approaches can provide complementary information by detecting selected resistance determinants alongside direct assessment of bacterial response to antibiotics; however, molecular panels are limited to their targets, and gene detection alone does not establish the expressed susceptibility phenotype. In proof-of-concept urine studies, a ready-to-use three-dimensional microwell array enabled direct single-cell AST and minimum inhibitory concentration assessment for *E. coli* in approximately three hours [46], while an enzyme-based on-filter method reported a sample-to-result time of about one hour after 20 min of antibiotic exposure [47]. If appropriately validated, such approaches could support earlier susceptibility-guided decisions. However, the cited urine-based studies primarily evaluated *E. coli*, and these technologies were not assessed in the present study. Their performance for *P. aeruginosa*, locally relevant antimicrobial agents, polymicrobial specimens, and clinical outcomes in Anbar requires further analytical and multicentre clinical validation. Rapid AST should therefore be viewed as a promising complement to, rather than a replacement for, standardized culture-based susceptibility testing.

5. Conclusions

Urinary *P. aeruginosa* isolates in this study displayed multidrug resistance and multiple virulence-associated traits. All 20 isolates met the study's MDR criterion and showed moderate-to-strong biofilm formation in the crystal violet assay. PCR detected *algD*, *lasR*, *oprD*, and *mexB* target regions in all isolates, although target detection alone does not establish gene expression or function. These findings support continued local surveillance, susceptibility-guided antimicrobial use, and effective infection-control practices.

Supplementary Materials: The following supporting information can be downloaded at: https://www.mdpi.com/article/10.3390/joma3020031/s1, Supplementary Table S1. Biochemical characterization of confirmed *P. aeruginosa* urinary isolates (PA1–PA20) compared with ATCC 15442 reference strain. Figure S1. Representative colony morphology of clinical urinary *P. aeruginosa* isolates grown on (A) blood agar, (B) MacConkey agar, and (C) cetrimide agar. These images are illustrative; isolate-level identification findings are summarized in the main manuscript. Figure S2. Representative Gram-stained preparation showing Gram-negative rod morphology (A) and a representative motility assessment (B). These images provide supplementary identification documentation; species confirmation was also supported by automated identification and 16S rRNA gene analysis, as described in the main manuscript. Figure S3. Phenotypic assays of urinary *P. aeruginosa* isolates: (a) extracellular polysaccharide detection; (b) protease activity; (c) lecithinase activity; and (d) coagulase activity using the tube method and slide method. Figure S4. Representative agar plates illustrating pyocin production by urinary *Pseudomonas aeruginosa* clinical isolates using the well-diffusion assay against *Staphylococcus aureus* ATCC 25923. Figure S5. Pyocin production by *P. aeruginosa* clinical isolates was determined using the well-diffusion method. Inhibition-zone diameters (mm) are presented as mean ± standard deviation from three independent replicates, with individual data points illustrating variability.

Author Contributions: M.I.M. was responsible for conceptualization, methodology, data collection, experimentation, data analysis, and drafting the manuscript. V.S. contributed to supervision, validation, interpretation of the results, and manuscript revision. P.P. participated in data analysis, and V.A.A. contributed to data interpretation and validation. M.M. assisted with manuscript revision and data interpretation. All authors have read and agreed to the published version of the manuscript.

Funding: This work was supported by the Indian Council for Cultural Relations [ICCR] under the Atal Bihari Vajpayee General Scholarship Scheme for the academic year 2023–2024 [Reference No. PC9239622970173].

Institutional Review Board Statement: Ethical approval for this study was granted by the Ethics Committee at the University of Anbar, Iraq, approval number 257, on 26 December 2024.

Informed Consent Statement: All participants were provided with clear information about the objectives of this study, and written informed consent was obtained from each patient before urine samples were collected, in accordance with ethical and institutional guidelines.

Data Availability Statement: The data presented in this study are available on request from the corresponding author due to patient confidentiality and ethical restrictions.

Acknowledgments: The authors acknowledge the Department of Biotechnology, Bharathiar University, for providing laboratory facilities and technical assistance throughout the study. During the preparation of this manuscript, AI-assisted tools (ChatGPT-5.3) were used solely for language editing and grammar improvement. All scientific content, experimental design, data analysis, and conclusions were developed independently by the authors. The authors have reviewed and edited the output and take full responsibility for the content of this publication.

Conflicts of Interest: The authors declare no conflicts of interest.

Abbreviations

ATCC	American Type Culture Collection
ANOVA	Analysis of variance
AK	amikacin
ATM	aztreonam
BHI	Brain heart infusion
CAZ	ceftazidime
CAUTI	Catheter-associated urinary tract infection
CFU	Colony-forming unit(s)
CIP	ciprofloxacin
CLSI	Clinical and Laboratory Standards Institute
CRA	Congo red agar
CV	Crystal violet
DNase	Deoxyribonuclease
MDR	Multidrug-resistant
MHA	Mueller-Hinton agar
MAR	Multiple antibiotic resistance
OD	Optical density
OprD	Outer membrane porin D
PBS	Phosphate-buffered saline
PRL	piperacillin
QS	Quorum sensing
SD	Standard deviation
TSI	Triple sugar iron
UTI	Urinary tract infection
VITEK	Automated microbial identification system

References

1. Flores-Mireles, A.L.; Walker, J.N.; Caparon, M.; Hultgren, S.J. Urinary tract infections: Epidemiology, mechanisms of infection and treatment options. *Nat. Rev. Microbiol.* **2015**, *13*, 269–284. [CrossRef] [PubMed]
2. Takeyama, K.; Kunishima, Y.; Matsukawa, M.; Takahashi, S.; Hirose, T.; Tsukamoto, T.; Kobayashi, N.; Kobayashi, I. Multidrug-resistant *Pseudomonas aeruginosa* isolated from the urine of patients with urinary tract infection. *J. Infect. Chemother.* **2002**, *8*, 59–63. [CrossRef] [PubMed]
3. Karruli, A.; Catalini, C.; D'Amore, C.; Foglia, F.; Mari, F.; Harxhi, A.; Galdiero, M.; Durante-Mangoni, E. Evidence-Based Treatment of *Pseudomonas aeruginosa* Infections: A Critical Reappraisal. *Antibiotics* **2023**, *12*, 399. [CrossRef] [PubMed]
4. Oliver, A.; Mulet, X.; López-Causapé, C.; Juan, C. The increasing threat of *Pseudomonas aeruginosa* high-risk clones. *Drug Resist Updat.* **2015**, *21–22*, 41–59. [CrossRef] [PubMed]
5. Elbehiry, A.; Marzouk, E.; Edrees, H.M.; Ibrahem, M.; Alzahrani, S.; Anagreyyah, S.; Abualola, H.; Alghamdi, A.; Alzahrani, A.; Jaber, M.; et al. Understanding *Pseudomonas aeruginosa* Biofilms: Quorum Sensing, c-di-GMP Signaling, and Emerging Antibiofilm Approaches. *Microorganisms* **2026**, *14*, 109. [CrossRef] [PubMed]
6. Qader, G.M.; Jarjees, K.K.; Jarjees, R.K. Molecular detection of metallo-beta-lactamase and alginate in multidrug-resistant *Pseudomonas aeruginosa* isolated from clinical specimens. *J. Med. Life* **2022**, *15*, 1105–1109. [CrossRef] [PubMed]
7. Eriksson, A.; Turkina, M.V.; Ntzouni, M.; Magnusson, K.E.; Vikström, E. *Pseudomonas aeruginosa* LasI/RhlI quorum sensing system controls protease-mediated autoaggregation behavior, cell envelope characteristics and extracellular proteome responses. *Front. Microbiol.* **2026**, *16*, 1693814. [CrossRef] [PubMed]
8. Pang, Z.; Raudonis, R.; Glick, B.R.; Lin, T.J.; Cheng, Z. Antibiotic resistance in *Pseudomonas aeruginosa*: Mechanisms and alternative therapeutic strategies. *Biotechnol. Adv.* **2019**, *37*, 177–192. [CrossRef] [PubMed]
9. Matsumoto, Y.; Yamasaki, S.; Hayama, K.; Iino, R.; Noji, H.; Yamaguchi, A.; Nishino, K. Changes in the expression of *mexB*, mexY, and oprD in clinical *Pseudomonas aeruginosa* isolates. *Proc. Jpn. Acad. Ser. B Phys. Biol. Sci.* **2024**, *100*, 57–67. [CrossRef] [PubMed]
10. Mudaliar, S.B.; Bharath Prasad, A.S. A biomedical perspective of pyocyanin from *Pseudomonas aeruginosa*: Its applications and challenges. *World J. Microbiol. Biotechnol.* **2024**, *40*, 90. [CrossRef] [PubMed]
11. Elbargisy, R.M. Characterization of Uropathogenic *Pseudomonas aeruginosa*: Serotypes, Resistance Phenotypes, and Virulence Genotypes. *J. Pure Appl. Microbiol.* **2022**, *16*, 1284–1297. [CrossRef]
12. Al-Orphaly, M.; Hadi, H.A.; Eltayeb, F.K.; Al-Hail, H.; Samuel, B.G.; Sultan, A.A.; Skariah, S. Epidemiology of Multidrug-Resistant *Pseudomonas aeruginosa* in the Middle East and North Africa Region. *mSphere* **2021**, *6*, e00202-21. [CrossRef] [PubMed]

13. Hussein, N.R.; Abozait, H.J.; Yasen, R.L.; Naqid, I.A. Antibiotic Resistance in *Pseudomonas aeruginosa* in Iraq: A Narrative Review. *J. Life Bio Sci. Res.* **2025**, *6*, 55–63. [CrossRef]
14. Bdawi, S.A.; Obaid, S.; Almawa, G.; Ayvaz, A. Profiling virulence genes in ceftazidime-resistant *Pseudomonas aeruginosa*: A comprehensive study across five hospitals in Iraq. *Pak. J. Pharm. Sci.* **2025**, *38*, 2342–2352. [CrossRef] [PubMed]
15. Mallikarjuna, P.V.; Dhanashree, B. Phenotypic and genotypic characterization of clinical *Pseudomonas aeruginosa*. *J. Taibah Univ. Med. Sci.* **2023**, *18*, 480–487. [CrossRef] [PubMed]
16. Qin, S.; Xiao, W.; Zhou, C.; Pu, Q.; Deng, X.; Lan, L.; Liang, H.; Song, X.; Wu, M. *Pseudomonas aeruginosa*: Pathogenesis, virulence factors, antibiotic resistance, interaction with host, technology advances and emerging therapeutics. *Signal Transduct. Target Ther.* **2022**, *7*, 199. [CrossRef] [PubMed]
17. Mutar, M.I.; Velayuthaprabhu, S.; Latef, S.A. Investigation of Silver Nanoparticles Synthesized by Galactose and Their Synergistic Antibacterial and Antibiofilm Activity with Gentamicin Against MDR *Pseudomonas aeruginosa* Isolates from UTI Patients. *Bionanoscience* **2026**, *16*, 359. [CrossRef]
18. Moehario, L.H.; Tjoa, E.; Putranata, H.; Joon, S.; Edbert, D.; Robertus, T. Performance of TDR-300B and VITEK® 2 for the identification of *Pseudomonas aeruginosa* in comparison with VITEK®-MS. *J. Int. Med. Res.* **2021**, *49*, 300060521989893. [CrossRef] [PubMed]
19. Geneaid Biotech Ltd. *DNA Isolation Kit (Bacteria): Quick Protocol*; Geneaid Biotech Ltd.: Taiwan, China, 2017; p. 150.
20. Li, M.N.; Han, Q.; Wang, N.; Wang, T.; You, X.M.; Zhang, S.; Zhang, C.-C.; Shi, Y.-Q.; Qiao, P.-Z.; Man, C.-L.; et al. 16S rRNA gene sequencing for bacterial identification and infectious disease diagnosis. *Biochem. Biophys. Res. Commun.* **2024**, *739*, 150974. [CrossRef] [PubMed]
21. Tamura, K.; Stecher, G.; Kumar, S. MEGA11: Molecular Evolutionary Genetics Analysis Version 11. *Mol. Biol. Evol.* **2021**, *38*, 3022–3027. [CrossRef]
22. Clinical and Laboratory Standards Institute (CLSI). *Performance Standards for Antimicrobial Susceptibility Testing*, 35th ed.; CLSI supplement M100; Clinical and Laboratory Standards Institute: Wayne, PA, USA, 2025.
23. Magiorakos, A.P.; Srinivasan, A.; Carey, R.B.; Carmeli, Y.; Falagas, M.E.; Giske, C.G.; Harbarth, S.; Hindler, J.F.; Kahlmeter, G.; Olsson-Liljequist, B.; et al. Multidrug-resistant, extensively drug-resistant and pandrug-resistant bacteria: An international expert proposal for interim standard definitions for acquired resistance. *Clin. Microbiol. Infect.* **2012**, *18*, 268–281. [CrossRef] [PubMed]
24. Quddus, S.; Liaqat, Z.; Azam, S.; Haq, M.U.; Ahmad, S.; Alharbi, M.; Khan, I. Identification of Efflux Pump Mutations in *Pseudomonas aeruginosa* from Clinical Samples. *Antibiotics* **2023**, *12*, 486. [CrossRef] [PubMed]
25. Stepanovic, S.; Vukovic, D.; Dakic, I.; Savic, B.; Svabic-Vlahovic, M. A modified microtiter-plate test for quantification of staphylococcal biofilm formation. *J. Microbiol. Methods* **2000**, *40*, 175–179. [CrossRef] [PubMed]
26. Stepanović, S.; Vuković, D.; Hola, V.; Di Bonaventura, G.; Djukić, S.; Cirković, I.; Ruzicka, F. Quantification of biofilm in microtiter plates: Overview of testing conditions and practical recommendations for assessment of biofilm production by staphylococci. *Apmis* **2007**, *115*, 891–899. [CrossRef] [PubMed]
27. Triveda, L.; Gomathi, S. Detection of biofilm formation among the clinical isolates of Enterococci: An evaluation of three different screening methods. *Int. J. Curr. Microbiol. Appl. Sci.* **2016**, *5*, 643–650. [CrossRef]
28. Fortuna, A.; Collalto, D.; Rampioni, G.; Leoni, L. Assays for Studying *Pseudomonas aeruginosa* Secreted Proteases. *Methods Mol. Biol.* **2024**, *2721*, 137–151. [CrossRef] [PubMed]
29. Teixeira, F.L.; Pauer, H.; Valente, G.L.C.; de Paula, G.R. Comparative analysis of virulence factors produced by *Pseudomonas aeruginosa* strains isolated from chronic wounds or bloodstream infections. *microPublication Biol.* **2024**, *2024*, 001413. [CrossRef] [PubMed]
30. Katz, D.S. *Coagulase Test Protocol*; ASM: Almere, The Netherlands, 2016; pp. 1–12.
31. Ridder, M.J.; Daly, S.M.; Hall, P.R.; Bose, J.L. Quantitative Hemolysis Assays. *Methods Mol. Biol.* **2021**, *2341*, 25–30. [CrossRef] [PubMed]
32. Fyfe, J.A.; Harris, G.; Govan, J.R. Revised pyocin typing method for *Pseudomonas aeruginosa*. *J. Clin. Microbiol.* **1984**, *20*, 47–50. [CrossRef] [PubMed]
33. Shouman, H.; Said, H.S.; Kenawy, H.I.; Hassan, R. Molecular and biological characterization of pyocyanin from clinical and environmental *Pseudomonas aeruginosa*. *Microb. Cell Fact.* **2023**, *22*, 166. [CrossRef] [PubMed]
34. Reyes, E.A.; Bale, M.J.; Cannon, W.H.; Matsen, J.M. Identification of *Pseudomonas aeruginosa* by pyocyanin production on Tech agar. *J. Clin. Microbiol.* **1981**, *13*, 456–458. [CrossRef] [PubMed]
35. Edén, C.S.; Hansson, H.A. *Escherichia coli* pili as possible mediators of attachment to human urinary tract epithelial cells. *Infect. Immun.* **1978**, *21*, 229–237. [CrossRef] [PubMed]
36. Reid, G.; Sobel, J.D. Bacterial adherence in the pathogenesis of urinary tract infection: A review. *Rev. Infect. Dis.* **1987**, *9*, 470–487. [CrossRef] [PubMed]
37. Silby, M.W.; Winstanley, C.; Godfrey, S.A.C.; Levy, S.B.; Jackson, R.W. Pseudomonas genomes: Diverse and adaptable. *FEMS Microbiol. Rev.* **2011**, *35*, 652–680. [CrossRef] [PubMed]

38. Weisburg, W.G.; Barns, S.M.; Pelletier, D.A.; Lane, D.J. 16S ribosomal DNA amplification for phylogenetic study. *J. Bacteriol.* **1991**, *173*, 697–703. [CrossRef] [PubMed]
39. Johnson, J.S.; Spakowicz, D.J.; Hong, B.Y.; Petersen, L.M.; Demkowicz, P.; Chen, L.; Leopold, S.R.; Hanson, B.M.; Agresta, H.O.; Gerstein, M.; et al. Evaluation of 16S rRNA gene sequencing for species and strain-level microbiome analysis. *Nat. Commun.* **2019**, *10*, 5029. [CrossRef] [PubMed]
40. Deschaght, P.; De Baere, T.; Van Simaey, L.; Van Daele, S.; De Baets, F.; De Vos, D.; Pirnay, J.-P.; Vaneechoutte, M. Comparison of the sensitivity of culture, PCR and quantitative real-time PCR for the detection of *Pseudomonas aeruginosa* in sputum of cystic fibrosis patients. *BMC Microbiol.* **2009**, *9*, 244. [CrossRef] [PubMed]
41. Feltner, J.B.; Wolter, D.J.; Pope, C.E.; Groleau, M.C.; Smalley, N.E.; Greenberg, E.P.; Mayer-Hamblett, N.; Burns, J.; Déziel, E.; Hoffman, L.R.; et al. LasR Variant Cystic Fibrosis Isolates Reveal an Adaptable Quorum-Sensing Hierarchy in *Pseudomonas aeruginosa*. *mBio* **2016**, *7*, e01513-16. [CrossRef] [PubMed]
42. Terzi, H.A.; Kulah, C.; Atasoy, A.R.; Ciftci, I.H. Investigation of OprD porin protein levels in carbapenem-resistant *Pseudomonas aeruginosa* isolates. *Jundishapur J. Microbiol.* **2015**, *8*, e25952. [CrossRef] [PubMed]
43. Krumperman, P.H. Multiple antibiotic resistance indexing of *Escherichia coli* to identify high-risk sources of fecal contamination of foods. *Appl. Environ. Microbiol.* **1983**, *46*, 165–170. [CrossRef] [PubMed]
44. Reszetnik, G.; Hammond, K.; Mahshid, S.; AbdElFatah, T.; Nguyen, D.; Corsini, R.; Caya, C.; Papenburg, J.; Cheng, M.P.; Yansouni, C.P. Next-generation rapid phenotypic antimicrobial susceptibility testing. *Nat. Commun.* **2024**, *15*, 9719. [CrossRef] [PubMed]
45. Bermudez, T.; Schmitz, J.E.; Boswell, M.; Humphries, R. Novel technologies for the diagnosis of urinary tract infections. *J. Clin. Microbiol.* **2025**, *63*, e00306-24. [CrossRef] [PubMed]
46. Wu, W.; Cai, G.; Liu, Y.; Suo, Y.; Zhang, B.; Jin, W.; Yu, Y.; Mu, Y. Direct single-cell antimicrobial susceptibility testing of *Escherichia coli* in urine using a ready-to-use 3D microwell array chip. *Lab Chip* **2023**, *23*, 2399–2410. [CrossRef] [PubMed]
47. Wu, W.; Suo, Y.; Zhao, Q.; Cai, G.; Liu, Y.; Jin, W.; Mu, Y.; Zhang, B. Inoculum size-insensitive susceptibility determination of urine sample based on in-situ measurement of inducible enzyme activity after 20 min of antibiotic exposure. *Anal. Chim. Acta* **2023**, *1282*, 341858. [CrossRef] [PubMed]

Disclaimer/Publisher's Note: The statements, opinions and data contained in all publications are solely those of the individual author(s) and contributor(s) and not of MDPI and/or the editor(s). MDPI and/or the editor(s) disclaim responsibility for any injury to people or property resulting from any ideas, methods, instructions or products referred to in the content.